*Desalination and Water Treatment*
www.deswater.com

doi: 10.1080/19443994.2016.1141377

57 (2016) 24278–24287
November

Taylor & Francis
Taylor & Francis Group

# Flux improvement of ultrafiltration membranes using ultrasound and gas bubbling

Masoud Hashemi Shahraki[a,*], Abdolmajid Maskooki[a], Ali Faezian[b], Ali Rafe[a]

[a]*Department of Food Processing, Research Institute of Food Science and Technology (RIFST), P.O. Box 91735-147, km 12, Asian Highway, Mashhad, Iran, Tel. +98 9381321295; Fax: +98 513 5003150; emails: m.hashemi.sh@gmail.com (M.H. Shahraki), a.maskooki@rifst.ac.ir (A. Maskooki), alirafe1400@yahoo.com (A. Rafe)*

[b]*Food Machinery Design Department, Research Institute of Food Science and Technology (RIFST), P.O. Box 91735-147, km 12, Asian Highway, Mashhad, Iran, Tel. +98 5135425330; Fax: +98 513 5003150; email: faezian@yahoo.com*

Received 10 July 2015; Accepted 9 January 2016

ABSTRACT

This study investigated the effects of ultrasound (US) and gas bubbling (GB) on permeate flux and membrane fouling. The ultrafiltration process of 1% skimmed milk was performed under various ultrasonic frequencies (37, 80 kHz, and tandem), irradiation modes (pulsed and sweeping), two-phase flow patterns (bubble and slug), and gas flow rates. The results showed that the US treatment improves the permeate flux up to 180%. The highest cleaning effect was obtained in the pulsed mode at 37 kHz. In the tandem frequency, the results showed that the fouling percentage significantly decreased with reduction in the frequency switching time. The GB injection treatment improved the mean of permeate flux up to 72% after 30 min. The slug pattern at medium gas flow rate was more effective than the other treatments. Best result was achieved in combination of the US (pulsed mode—37 kHz) and the GB (slug pattern—medium flow rate). In this condition, the permeate flux was significantly improved up to 384% in comparison with the control. Furthermore, the hydrodynamic resistance results showed the higher ability of the US in cleaning of membrane pores during ultrafiltration.

*Keywords:* Fouling; Ultrafiltration; Gas bubbling; Ultrasound

## 1. Introduction

The widespread application of membrane technology has been a result of its growing industrial purposes. However, the development of membrane technology has been limited due to the flux decline during separation process [1–4]. The decline in flux is commonly concerned to the concentration polarization and fouling [5,6]. The phenomenon of fouling is due to the concentration polarization and settling of organic and inorganic materials in feed on active surface and pores of the membrane during the separation process [7]. In this situation, the concentration of the rejected material on the membrane surface increased and afterward the permeate flux gradually decreased. The concentration polarization was completely different from fouling, as concentration polarization has no permanent effect on the membrane itself and can be reversed by creating turbulence in feed flow during membrane filtration, whereas fouling is due to blockage of membrane pores [1,6].

*Corresponding author.

Many cleaning techniques are being applied to reduce fouling and cleaning of membrane such as chemical and biochemical cleaning [8], which has limitations, including the damage of the membrane, and cause secondary pollution by chemical cleaning [9]. Several techniques have been used to prevent flux decline during membrane filtration [10–16]: pretreatment of the feed [11], manipulation of cross-flow (turbulence promotion, back-flushing, and pulsing) [6,12], shear-enhanced filtration (rotating disk and rotating membranes) [13], filtration under electric and ultrasonic fields [14,15,17], and gas bubbling (GB) [1,3].

Among the novel physical methods, power ultrasound (US) has been interested more than the other methods [18–20]. The ultrasound-assisted techniques provide an alternative method for membrane fouling control and cleaning [17,21], as well as for the characterization of membrane fouling [22]. The effect of the US is based on detaching the foulants by cavitation and microstream mechanisms [23]. The cavitation phenomena are the result of growth and implosion collapse of bubbles which occurred when a large negative pressure is applied to a liquid medium. Microstreaming is defined as the fluid circulation near cavitation bubbles, which generated by the oscillation of bubble size during compression and rarefaction cycles, and microstreamers refer to the bubbles that travel to a mutual "node" or "antinode" in the fluid [24].

Inducing turbulence in the vicinity of membrane surface with an increase in cross-flow velocity is a major strategy to promote mass transfer. However, increasing the cross-flow velocity to obtain more turbulent flow is not always efficient and it has drawbacks like increasing energy consumption [25]. A desirable method to increase turbulence is by providing gas/liquid two-phase flow with injection of gas into the feed flow. Air bubbling has been extensively applied to prevent deposition of particles on membrane surfaces and eliminate deposited material from the membrane surface by increasing turbulence and shear stress [1,3,16,20].

Although many studies have investigated the influence of low frequencies of US and GB on the detaching process of membrane foulants separately, the combination effect of the sonication modes and the flow pattern on flux improvement have not been evaluated. Hence, the purpose of this work is to study the interaction effects of the sonication modes and the GB flow pattern on the permeation flux of the ultrafiltration process.

## 2. Materials and methods

### 2.1. Materials

Skimmed milk powder was purchased from the local market and used as feed with 1 wt% solid content concentration in ultrafiltration processing. The temperature of feed was fixed at 20 ± 2˚C during the separation process. The physicochemical properties of skimmed milk is shown in Table 1.

Flat sheet polyethersulfone ultrafiltration membrane (Sepro Company, USA), with 10 KD molecular weight cut off was used in Minitan S (Millipore Inc.) system. The effective membrane area was 112 $cm^2$. The membrane was placed between the two silicon separator of 1 mm thickness and two acrylic manifolds of thickness 2.3 cm, which were in turn held in place by stainless steel plates of 1.1 cm thickness, according to instruction of using Minitab S by Millipore. The integrity test (pressure decay test) was performed for each new membrane to ensure the lack of leakage before the experiment [26]. The liquid nitrogen with a purity of 99.97% was supplied by Tous Gas Company, Mashhad, Iran.

### 2.2. Methods

#### 2.2.1. Ultrafiltration

The experimental setup is shown in Fig. 1. The system consists of a flat-sheet membrane and a connected feed tank to a peristaltic pump. This pump supplies a sufficient and constant pressure. All the experimental tests were carried out for 30 min in a fixed 3 bar inlet pressure and at 20 ± 2˚C temperature. The membrane was renewed for each experiment. The differences between inlet and outlet pressure of the feed ($\Delta P$) were measured by two mounted pressure gauges in the feed line before and after of the flat module. One pressure gauge was also inserted on the permeate flux outlet. During the fouling process, permeate and retentate were recycled to the feed tank to maintain the constant feed concentration. The viscosity of permeate was measured by Brookfield Viscometer Tokimec (Model BL, USA).

#### 2.2.2. Sonication

The flat-sheet membrane module was directly located in an ultrasonic bath (Model Elmasonic, Germany) with dimension of 200 mm × 300 mm × 505 mm and 30 L capacity, which is connected to the temperature control circulator. The membrane unit is kept 10 cm above the bottom and 13 cm far from the transducers. The power of sonicator was 380 W.

Table 1
Physicochemical properties of skimmed milk (1 wt%) as feed sample

| Ash (kg/100 kg) | Lactose (kg/100 kg) | Protein (kg/100 kg) | Density ($kg/m^3$) | Viscosity (Pa.s) | Conductivity (S/m) | Brix (%) | TDS (ppm) | pH | Particle size of powder (m) |
|---|---|---|---|---|---|---|---|---|---|
| 0.00721 | 0.04657 | 0.03035 | 1,032 | $1.47 \times 10^{-3}$ | $9.1 \times 10^{-2}$ | 1.11 | 460 | 6.93 | $0.2–2.5 \times 10^{-4}$ |

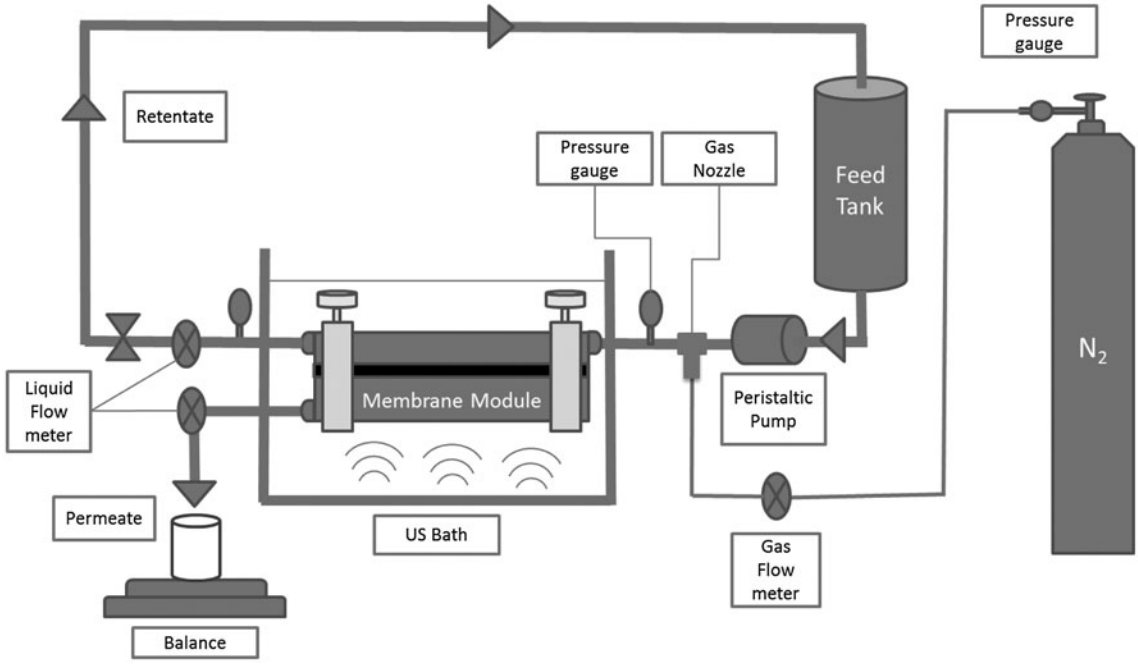


Fig. 1. Schematic of ultrafiltration setup assisted with ultrasonic cleaner bath and GB system.

The sonication experiments were performed at 37, 80 kHz, and tandem (switch between 37 and 80 kHz alternatively for each 1minute) frequencies with sonic power 100% in the pulsed and sweeping modes of US irradiation. In the pulsed mode, the power of US increased by 20% at fixed frequency. In the sweeping mode, a more homogenous sounding of the bath is achieved by the continuous ascending displacement of the sound pressure amplitude in the cleaning liquid. The temperature of ultrasonic bath was fixed at 30 ± 1°C by water circulating system [17].

In order to confirm the cavitation existence in the test section, an aluminum foil was placed between two manifolds instead of membranes and then immersed in an ultrasonic bath, and US excitation is executed same as main tests. These experiments were performed under no pressure [27]. In this test, many holes appeared on the aluminum foil that indicates the US treatments led to perforation of the foil due to cavitation effects. In order to find out the possible damages to the membranes which were exposed to the US energy, the hydrodynamic resistances were evaluated for new membranes with deionized water before and after the US treatments [28].

### 2.2.3. Gas bubbling

The pure nitrogen gas is injected directly to the feed to perform GB treatment (Fig. 1). GB was performed in the bubble and slug flow pattern (Fig. 2). In the bubble pattern, the length scale of gas bubble is less than (e.g. <60%) the tube diameter. Slug flow (also called plug flow) occurs, when the bullet-shaped bubbles of gas approach the diameter of the tube in the fluid bed [16]. The gas–liquid two-phase flow pattern depends on the gas injection factor ($r$), which equals

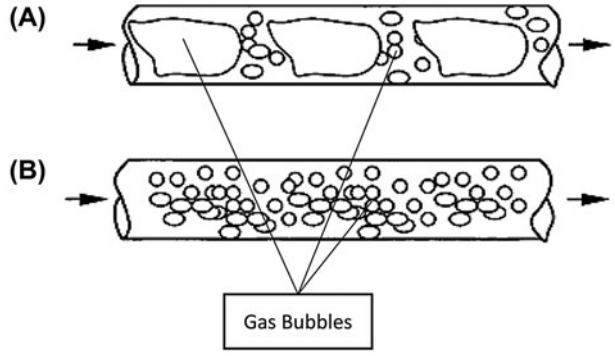


Fig. 2. GB two-phase flow patterns: (A) Slug pattern and (B) Bubble pattern.

to Ug/(Ug + Ul). Ug and Ul are the superficial gas and liquid flow rate or flow velocity, respectively. The two-phase flow pattern changes from bubble flow ($0 < r < 0.2$) over slug flow ($0.2 < r < 0.9$) to annular flow ($0.9 < r < 1.0$) [29]. The gas was set at three flow rates (as low, medium, and high): 0.5, 1, and 1.5 L $min^{-1}$ for slug flow and 0.1, 0.2, and 0.3 L $min^{-1}$ for the bubble flow pattern. The length scale of slug pattern approached to the diameter of the gas feeding nozzle. The gas was injected into the main fluid flow through the branch of the simple *T*-shaped Junction.

#### 2.2.4. Parameters calculation

Transmembrane pressure is calculated by Eq. (1).

$$\Delta P = \left[(P_f + P_r) \cdot 2^{-1}\right] - P_p \quad (1)$$

where ($\Delta P$) is the transmembrane pressure (Pa), $P_f$ is the feed pressure (Pa), $P_r$ is the retentate pressure (Pa), and $P_p$ is the permeate pressure (Pa).

The permeate flux is measured using Eq. (2) [28]:

$$J = (W_{ti} - W_{ti-1}) \cdot (d \cdot \Delta t)^{-1} \quad (2)$$

where $J$ is the permeate flux ($m^3\ m^{-2}\ s^{-1}$), $W_{ti}$ is the permeate weight at time $i$ (kg), $W_{ti-1}$ is the permeate weight at time i–1 (kg), $d$ is the density of permeate (kg $m^{-3}$), and $\Delta t$ (s) is the time interval.

The hydrodynamic resistance is calculated by Eq. (3).

$$R_H = \Delta P \cdot (\mu \cdot J)^{-1} \quad (3)$$

where, $R_H$ is the hydrodynamic resistance (1 $m^{-1}$), $\Delta P$ is the steady-state system pressure, $\mu$ is the permeate viscosity (Pa.s), and $J$ is the permeate flux.

The resistance of cake layer is calculated by determining the difference amount of membrane resistance before and after removing the cake layer [1]. The total hydrodynamic resistance is calculated by the following Eq. (4):

$$R_t = R_m + R_c + R_f \quad (4)$$

where $R_t$ is the total hydrodynamic resistance, $R_m$ is the new membrane resistance, $R_c$ is the cake resistance, and $R_f$ is the fouling resistance.

The enhancement factor on the permeate flux is calculated and defined by Eq. (5):

$$EF\% = \left[(J_{us,gb} - J) \cdot J^{-1}\right] \times 100 \quad (5)$$

where $J_{us,gb}$ is the permeate flux of combined US and GB treatment, and $J$ is the intact permeate flux (without treatment).

The differences between deionized water flux before and after membrane fouling per deionized water flux of clean membrane is represented as fouling percent and is calculated by the following Eq. (6):

$$Fouling\% = \left[1 - \left(J_{wp} \cdot J_w{}^{-1}\right)\right] \times 100 \quad (6)$$

where $J_{wp}$ and $J_w$ are the permeate flux of membrane after and before fouling, respectively.

In order to evaluate the fouling, foulant weight is detected after 30 min ultrafiltration by Eq. (7):

$$\text{Foulant weight} = \text{membrane weight before filtration} - \text{dried membrane after filtration} \quad (7)$$

#### 2.2.5. Statistical analysis

Each treatment is carried out at least three times. The acquired raw data statistically are analyzed using multifactor Design in ANOVA table. The least significant differences are calculated and the mean values obtained are evaluated by Duncan's multiple range test. SigmaStat 3.1 and Microsoft EXCEL softwares are employed for statistical analysis.

## 3. Results and discussion

### 3.1. US treatment

The permeate flux under different frequencies of US in comparison with the control during 30 min ultrafiltration is shown in Fig. 3. As it can be found, change in the US frequency had a significant effect on the permeate flux. As the US frequencies were reduced, the permeate flux was increased. At low frequency, the compression (and rarefaction) cycles are long enough to grow the bubble to a sufficient size that causes the disruption of the liquid [30]. As a result, the lower US frequencies had higher cleaning efficiencies than that of the higher ones. In the low frequency of US, the turbulence, near the membrane surface, is more significant than the higher frequencies. Therefore, concentration polarization is reduced and leads to improvisation of the ultrafiltration flux [30,31]. The average permeate flux under the US treatment was $7.01 \times 10^{-6}$ in comparison with control ($2.5.10^{-6}$), which means the US treatment can improve the permeate flux up to 180%.

As shown in Fig. 3, the best permeate flux was obtained in the pulsed mode. In the pulsed mode, the power intensity of US waves was increased regularly about 20% at fixed frequency. In this condition, the number of cavitation bubbles increased with fixed size [5]. Thus, the cleaning effect could be increased due to more turbulence [17].

Our results showed that there is no significant difference ($p \geq 0.05$) between the frequency 37 kHz and the tandem mode of US, when 1 min was used as frequency switching time interval between 37 and 80 kHz. For more confirmation, shorter time interval of frequencies switching are evaluated. It was indicated that the maximum effect of US in the tandem mode was achieved only in 5 s and fouling percentage significantly increased with increasing time interval (Fig. 4). Gonzalez-Avila and coworkers have reported that the high frequency produces nucleate bubbles, and switching to low frequency led to induce a concerted collapse [32]. Changing the frequencies of US in the tandem mode acts as a shock in the vicinity of the membrane surface and as a result more turbulent occurs by the reducing of frequency switching time interval. On the other hand, it seems that the bubbles created by cavitation at frequency 37 kHz of US lead to mechanical removing of deposited materials and thus prevent the membrane surface fouling. In contrast, the bubbles that were created at 80 kHz are smaller than that at 37 kHz, and may penetrate to the pores of the membrane and remove the sedimentations in pores. In addition, regular changing of input waves or the tandem mode of US has led to regular resize of the cavitation bubble, and led to more turbulence near the vicinity of the membrane and active zones of separation. Maskooki and coworkers have used a tandem ultrasonic in order to clean the microfiltration membrane and they found the same results [33].

### 3.2. GB treatment

The effect of GB on the flux is demonstrated in Fig. 5. The GB treatment improved the mean permeate flux up to 72% in 30 min. The ultrafiltration

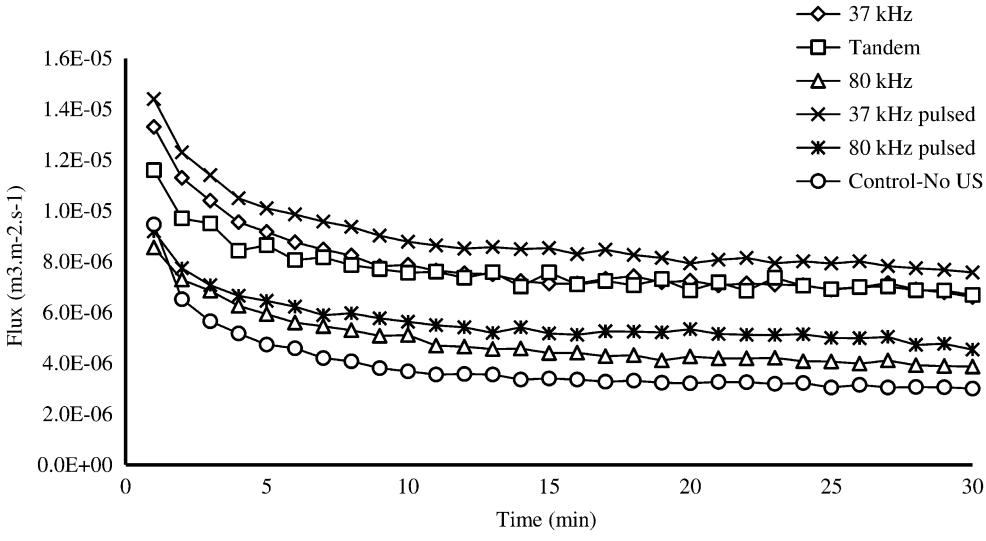


Fig. 3. The permeate flux rate under different frequencies of US compared to control during 30 min ultrafiltration.

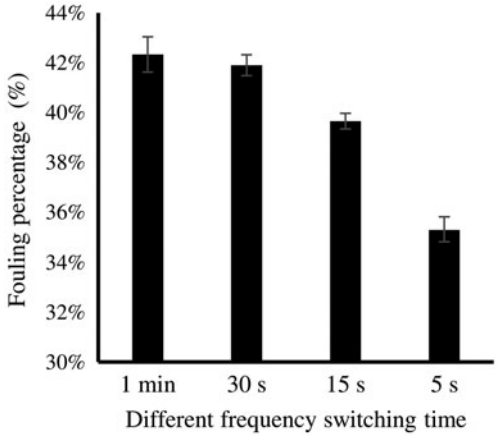


Fig. 4. The final fouling percentage of membrane for tandem mode with different time intervals of frequency switching.

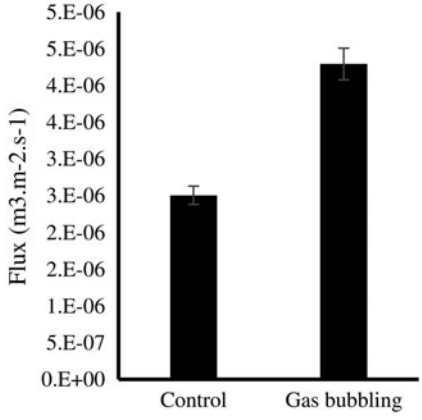


Fig. 5. Comparison of permeation flux mean under GB treatment with control after 30 min ultrafiltration, the permeation flux for GB is mean of permeation flux under $N_2$ bubbling.

performance is significantly influenced by the concentration polarization and subsequent fouling. Using surface shear is a major strategy to control these phenomena. The surface shear can also be enhanced by the two-phase flow [20]. The main mechanism that leads to increase in the surface shear is secondary flow, such as wakes and vortex [16].

The two-phase flow pattern influence on the permeate flux rate is shown in Fig. 6. As it can be seen, the slug pattern is more effective than the bubble pattern. Furthermore, larger bubbles are more effective than the smaller ones in promoting local mixing, due to the larger wake regions and creating stronger secondary flows [16]. Ndinisa and coworkers have reported that the fouling reduction improved with increasing size of gas injection system nozzle in submerged flat-sheet membranes [25].

It can be found from Fig. 7 that the permeate flux improved with the increasing gas flow rate until medium flow rate as an optimum value in the slug pattern. The shear intensity, which is linked to the GB is improved with the increasing gas flow rate. High shear forces may result in foulant removal from the membrane surface. Thus, a higher gas flow rate creates a two-phase flow, which is more beneficial for fouling control than the lower one [34,35]. Qaisrani et al. explained this phenomenon with bubble size and air flow rate relationship. Bubble size is directly proportion to the air flow rate. Therefore, bubble diameter increased with the increasing air flow rate. When the air flow rate became more than the optimum one, 1 L $min^{-1}$, it seems that the bubbles size becomes so great. Large bubbles hinder the liquid to reach the membrane surface. Hence, the bubbles act as cushions along the membrane surface and the permeate flux decreased with the increasing air flow rate [20].

### 3.3. US and GB combination

The best results obtained from a combination of the optimum conditions of the US and the GB treatments, are shown in Fig. 8. The combination of the pulsed 37 kHz of US and the slug flow pattern at the medium gas flow rate improved the mean permeate flux up to 384%. As mentioned, the pulsed 37 kHz of US and the slug flow pattern in the medium gas flow rate improved the mean permeate flux up to 181 and 72%, respectively.

Fluctuation at the optimum condition graph (37 kHz-pulsed, low-slug) has indicated cleaning effect of US and GB by removing some part of the cake layer from the membrane surface. A higher concentration polarization may cause a higher rate in the formation of the cake layer and therefore, the reducing of flux occurs faster during filtration with non-turbulent flow. In this condition, the gas bubble can increase the turbulence near the membrane surface. Furthermore, the shearing force of the gas bubbles can remove the cake layer from the membrane surface as discussed before. From the microscopic aspect, the generated cavitation by US waves, led to crack the cake layer and help the gas bubble to detach the foulant from the membrane surface.

Rooze et al. have reported some kind of interaction between US and GB that led to an increase in cleaning effect of US treatment [36]. Cleaning of the particles

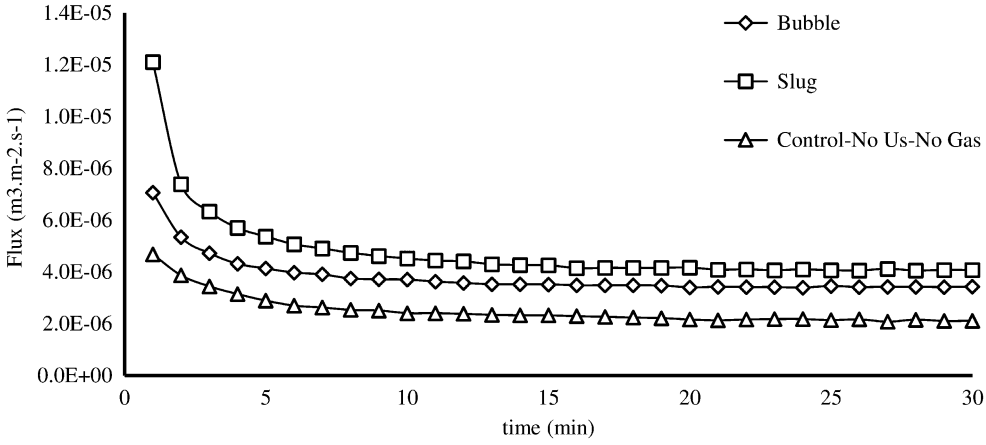


Fig. 6. Permeate flux under different two-phase patterns compared to control, during 30 min ultrafiltration.

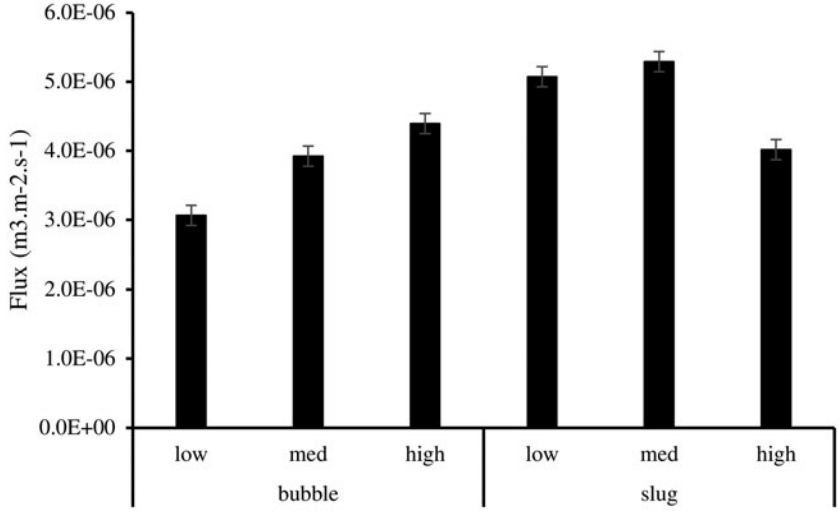


Fig. 7. Effect of different levels of gas flow rate on mean of permeate flux after 30 min ultrafiltration under GB with various two-phase flow patterns.

adhered to a surface is achieved by shear forces, which are available by oscillating the bubble cavitation near a wall. In this mechanism, fluid is sucked toward, and ejected away from the bubble and from the wall in a sweeping mode [37]. Degasification of the liquid decreases this process. Hauptmann et al. have applied an acoustic pressure to a cleaner jet and found the highest cleaning efficiency with oxygen at upper saturation [38].

In order to confirm the results, the foulant was weighed after ultrafiltration in a constant area of treated membranes. As it can be seen in Fig. 9, the foulant weight was the lowest under 37 kHz pulsed of the US and GB in the slug mode with medium flow rate that it shows the highest cleaning effect under this condition. The obtained *R*-square (0.8802) between permeate flux and foulant weight approves the results.

### 3.4. Hydrodynamic resistance

In order to evaluate the reversible and irreversible membrane fouling, the hydrodynamic resistances were evaluated after ultrafiltration. Fouling can be divided into irreversible and reversible fouling based on the attachment strength of particles to the membrane surface. Reversible fouling can be removed by a strong shear force. Sedimentation of the foulant within the membrane pores and formation of a strong matrix of fouling layer during a continuous filtration process

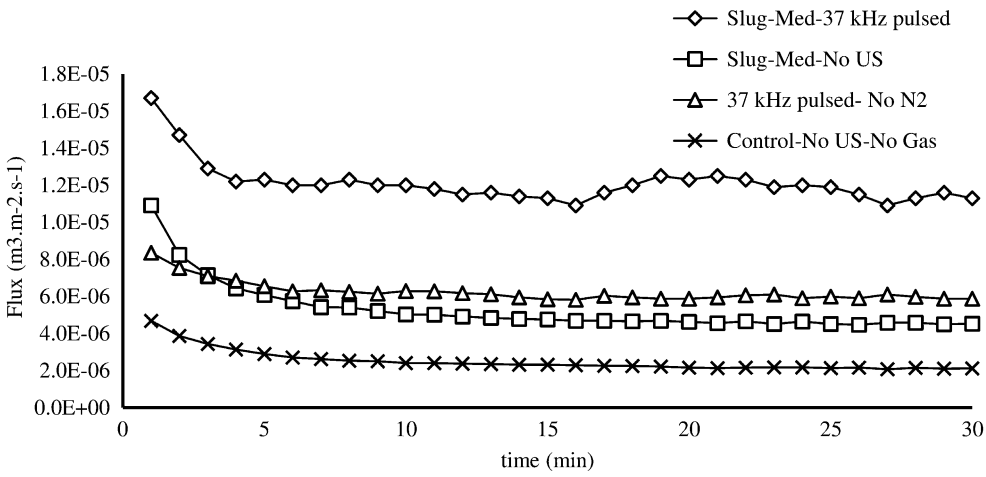


Fig. 8. Flux permeation under US and $N_2$-bubbling combination compared to the best obtained result of $N_2$ bubbling and US treatments, separately.

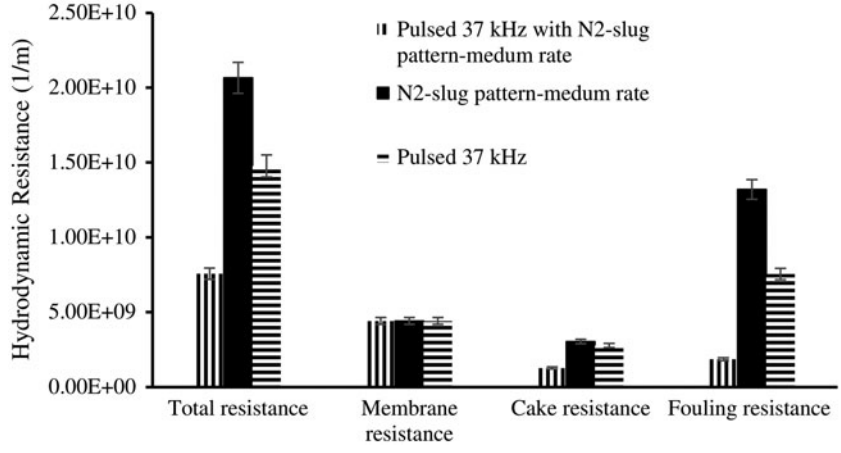


Fig. 9. Hydrodynamic resistances of membrane under the best condition of US, GB, and their combination, after 30 min ultrafiltration.

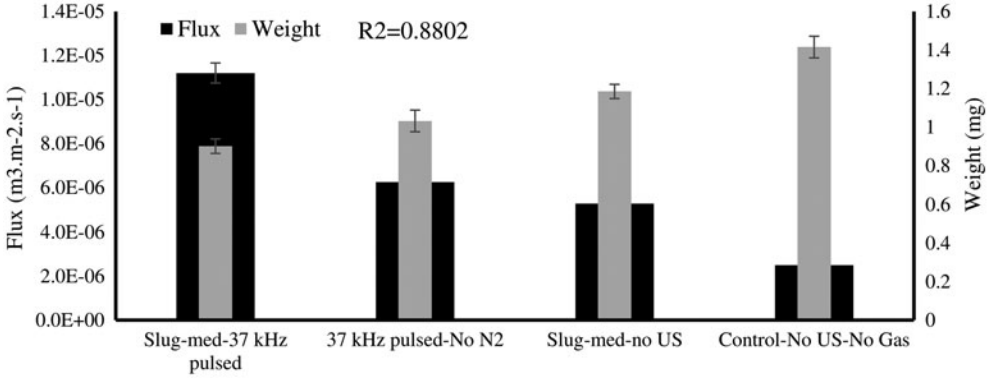


Fig. 10. Comparison of the weight of foulant and mean of permeation flux for the same membrane, under different US and GB treatments after 30 min.

will result in reversible fouling being transformed into an irreversible fouling layer. Irreversible fouling is the strong attachment of particles which cannot be removed by physical cleaning [1,22]. The ability of studied treatments in removing the cake layer (reversible) and cleaning or prevention of foulant sedimentation within the pores and formation of a strong matrix of fouling layer (irreversible) was evaluated during ultrafiltration process. The results for hydrodynamic resistance of the optimum conditions of US, GB, and their combination are shown in Fig. 10. The obtained total hydrodynamic resistances results confirmed the flux permeation results during filtration. With respect to Fig. 10, the cake resistance under the optimum conditions of the GB and the US showed no significant difference that indicated same ability for both the treatments in removing cake layer. The obtained fouling resistance in the optimum conditions of US was lower than the GB one. It could be concluded that the US can clean the pores better than the $N_2$-bubbling treatment.

## 4. Conclusion

The effects of US and GB injection treatment were investigated. The US significantly increased the permeate flux up to 180% in comparison with control. The highest cleaning of membrane foulant was also obtained in the pulsed irradiation mode of US. Our results showed that 5 s switching time between frequencies is enough for cleaning efficiency in the tandem mode and by increasing the time of switching on periodically, the fouling percentage was significantly increased. The GB treatment improved the mean flux up to 72% in 30 min. The slug mode as GB pattern in the medium flow rate is more effective than the bubble mode in cleaning of membrane foulant. The combination of pulsed 37 kHz and slug pattern in the medium gas flow rate improved the mean permeate flux up to 384% in comparison with control.

## Acknowledgment

The authors acknowledge Iran National Science Foundation (INSF) and Research Institute of Food Science and Technology (RIFST) for financial support.

## References

[1] A. Maskooki, M.H. Shahraki, M. Mohamadi, Effects of various frequencies and powers of ultrasound on cleaning of flat sheet membrane during and after microfiltration, Desalin. Water Treat. (in press) 1–9, doi: 10.1080/19443994.2014.1003978.

[2] S. Muthukumaran, S.E. Kentish, G.W. Stevens, M. Ashokkumar, Application of ultrasound in membrane separation processes: A review, Rev. Chem. Eng. 22 (2006) 155–194.

[3] M. Hashemi Shahraki, A. Maskooki, A. Faezian, Hollow fibers filtration and cleaning processes under ultrasound and gas bubbling combination, J. Food Process Eng (in press) 1–9, doi: 10.1111/jfpe.12325.

[4] J. Soler-Cabezas, M. Torà-Grau, M. Vincent-Vela, J. Mendoza-Roca, F. Martínez-Francisco, Ultrafiltration of municipal wastewater: Study on fouling models and fouling mechanisms, Desalin. Water Treat. 56 (2015) 3427–3437.

[5] H. Kyllönen, P. Pirkonen, M. Nyström, Membrane filtration enhanced by ultrasound: A review, Desalination 181 (2005) 319–335.

[6] M. Hashemi Shahraki, A. Maskooki, A. Faezian, Effect of soluble and insoluble gas bubbling methods on ultrafiltration fouling control, Desalin. Water Treat. (in press) 1–9, doi: 10.1080/19443994.2015.1123199.

[7] E. Matthiasson, B. Sivik, Concentration polarization and fouling, Desalination 35 (1980) 59–103.

[8] A. Ahmad, N.M. Yasin, C. Derek, J. Lim, Chemical cleaning of a cross-flow microfiltration membrane fouled by microalgal biomass, J. Taiwan Inst. Chem. Eng. 45 (2014) 233–241.

[9] J.P. Chen, S. Kim, Y. Ting, Optimization of membrane physical and chemical cleaning by a statistically designed approach, J. Membr. Sci. 219 (2003) 27–45.

[10] H. Ma, C.N. Bowman, R.H. Davis, Membrane fouling reduction by backpulsing and surface modification, J. Membr. Sci. 173 (2000) 191–200.

[11] S. Kim, J.P. Chen, Y. Ting, Study on feed pretreatment for membrane filtration of secondary effluent, Sep. Purif. Technol. 29 (2002) 171–179.

[12] H. Choi, K. Zhang, D.D. Dionysiou, D.B. Oerther, G.A. Sorial, Influence of cross-flow velocity on membrane performance during filtration of biological suspension, J. Membr. Sci. 248 (2005) 189–199.

[13] M.Y. Jaffrin, Dynamic shear-enhanced membrane filtration: A review of rotating disks, rotating membranes and vibrating systems, J. Membr. Sci. 324 (2008) 7–25.

[14] J.-P. Chen, C.-Z. Yang, J.-H. Zhou, X.-Y. Wang, Study of the influence of the electric field on membrane flux of a new type of membrane bioreactor, Chem. Eng. J. 128 (2007) 177–180.

[15] M. Smythe, R. Wakeman, The use of acoustic fields as a filtration and dewatering aid, Ultrasonics 38 (2000) 657–661.

[16] Z. Cui, S. Chang, A. Fane, The use of gas bubbling to enhance membrane processes, J. Membr. Sci. 221 (2003) 1–35.

[17] M.H. Shahraki, A. Maskooki, A. Faezian, Effect of various sonication modes on permeation flux in cross flow ultrafiltration membrane, J. Environ. Chem. Eng. 2 (2014) 2289–2294.

[18] A. Cerón-Vivas, J. Morgan-Sagastume, A. Noyola, Intermittent filtration and gas bubbling for fouling reduction in anaerobic membrane bioreactors, J. Membr. Sci. 423 (2012) 136–142.

[19] G. Chen, X. Yang, R. Wang, A.G. Fane, Performance enhancement and scaling control with gas bubbling in direct contact membrane distillation, Desalination 308 (2013) 47–55.

[20] T. Qaisrani, W. Samhaber, Impact of gas bubbling and backflushing on fouling control and membrane cleaning, Desalination 266 (2011) 154–161.
[21] D. Chen, L.K. Weavers, H.W. Walker, Ultrasonic control of ceramic membrane fouling by particles: Effect of ultrasonic factors, Ultrason. Sonochem. 13 (2006) 379–387.
[22] H. Choi, K. Zhang, D.D. Dionysiou, D.B. Oerther, G.A. Sorial, Effect of permeate flux and tangential flow on membrane fouling for wastewater treatment, Sep. Purif. Technol. 45 (2005) 68–78.
[23] J. Li, R.D. Sanderson, E.P. Jacobs, Ultrasonic cleaning of nylon microfiltration membranes fouled by Kraft paper mill effluent, J. Membr. Sci. 205 (2002) 247–257.
[24] Y. Gao, D. Chen, L.K. Weavers, H.W. Walker, Ultrasonic control of UF membrane fouling by natural waters: Effects of calcium, pH, and fractionated natural organic matter, J. Membr. Sci. 401 (2012) 232–240.
[25] N. Ndinisa, A. Fane, D. Wiley, Fouling control in a submerged flat sheet membrane system: Part I–bubbling and hydrodynamic effects, Sep. Sci. Technol. 41 (2006) 1383–1409.
[26] H. Guo, Y. Wyart, J. Perot, F. Nauleau, P. Moulin, Low-pressure membrane integrity tests for drinking water treatment: A review, Water Res. 44 (2010) 41–57.
[27] S. Muthukumaran, S. Kentish, S. Lalchandani, M. Ashokkumar, R. Mawson, G.W. Stevens, F. Grieser, The optimisation of ultrasonic cleaning procedures for dairy fouled ultrafiltration membranes, Ultrason. Sonochem. 12 (2005) 29–35.
[28] A. Mirzaie, T. Mohammadi, Effect of ultrasonic waves on flux enhancement in microfiltration of milk, J. Food Eng. 108 (2012) 77–86.
[29] W. Youravong, Z. Li, A. Laorko, Influence of gas sparging on clarification of pineapple wine by microfiltration, J. Food Eng. 96 (2010) 427–432.
[30] M.O. Lamminen, H.W. Walker, L.K. Weavers, Mechanisms and factors influencing the ultrasonic cleaning of particle-fouled ceramic membranes, J. Membr. Sci. 237 (2004) 213–223.
[31] T. Kobayashi, T. Kobayashi, Y. Hosaka, N. Fujii, Ultrasound-enhanced membrane-cleaning processes applied water treatments: Influence of sonic frequency on filtration treatments, Ultrasonics 41 (2003) 185–190.
[32] S.R. Gonzalez-Avila, F. Prabowo, A. Kumar, C.-D. Ohl, Improved ultrasonic cleaning of membranes with tandem frequency excitation, J. Membr. Sci. 415 (2012) 776–783.
[33] A. Maskooki, T. Kobayashi, S.A. Mortazavi, A. Maskooki, Effect of low frequencies and mixed wave of ultrasound and EDTA on flux recovery and cleaning of microfiltration membranes, Sep. Purif. Technol. 59 (2008) 67–73.
[34] Z. Ding, L. Liu, Z. Liu, R. Ma, The use of intermittent gas bubbling to control membrane fouling in concentrating TCM extract by membrane distillation, J. Membr. Sci. 372 (2011) 172–181.
[35] J.-Y. Tian, Y.-P. Xu, Z.-L. Chen, J. Nan, G.-B. Li, Air bubbling for alleviating membrane fouling of immersed hollow-fiber membrane for ultrafiltration of river water, Desalination 260 (2010) 225–230.
[36] J. Rooze, E.V. Rebrov, J.C. Schouten, J.T. Keurentjes, Dissolved gas and ultrasonic cavitation–A review, Ultrason. Sonochem. 20 (2013) 1–11.
[37] P. Marmottant, M. Versluis, N. de Jong, S. Hilgenfeldt, D. Lohse, High-speed imaging of an ultrasound-driven bubble in contact with a wall: "Narcissus" effect and resolved acoustic streaming, Exp. Fluids 41 (2006) 147–153.
[38] M. Hauptmann, S. Brems, E. Camerotto, A. Zijlstra, G. Doumen, T. Bearda, P. Mertens, W. Lauriks, Influence of gasification on the performance of a 1 MHz nozzle system in megasonic cleaning, Microelectron. Eng. 87 (2010) 1512–1515.